Organic Electronics 13 (2012) 2333–2341

Contents lists available at SciVerse ScienceDirect

Organic Electronics

journal homepage: www.elsevier.com/locate/orgel

Comparative study of spectral and morphological properties of blends of P3HT with PCBM and ICBA

You-Heng Lin [a], Yu-Tang Tsai [a], Chung-Chih Wu [a,*], Chih-Hung Tsai [b], Chien-Hung Chiang [c], Hsiu-Fu Hsu [c], Jey-Jau Lee [d], Ching-Yuan Cheng [d]

[a] Graduate Institute of Photonic and Optoelectronics, Department of Electrical Engineering, Graduate Institute of Electronics Engineering, and Innovative Photonics Advanced Research Center (i-PARC), National Taiwan University, Taipei 10617, Taiwan, ROC
[b] Department of Opto-Electronic Engineering, National Dong Hwa University, Hualien 97401, Taiwan, ROC
[c] Department of Chemistry, Tamkang University, Taipei 25137, Taiwan, ROC
[d] National Synchrotron Radiation Research Center (NSRRC), Hsin-Chu 30076, Taiwan, ROC

ARTICLE INFO

Article history:
Received 21 June 2012
Received in revised form 13 July 2012
Accepted 15 July 2012
Available online 1 August 2012

Keywords:
GIXS
Polymer solar cells
Fullerene
Poly(3-hexylthiophene)
Morphology

ABSTRACT

We report a comparative study on spectral and morphological properties of two blend systems for polymer solar cells: the donor material poly(3-hexylthiophene) (P3HT) in combination with the acceptor material of either [6,6]-phenyl-C_{61} butyric acid methyl ester (PCBM) or indene-C_{60} bisadduct (ICBA) that was reported to enhance efficiencies of polymer solar cells. Optical microscopy and grazing incidence X-ray scattering reveal the stronger tendency of PCBM to from larger and more ordered domains/grains than ICBA either in pure or blend films. Compared to PCBM, the presence of ICBA also substantially perturbs the organization and longer-range ordering of P3HT in increasing the ICBA ratio in blends. With larger and more ordered phase-separated domains, the P3HT/PCBM blend films exhibit significant optical scattering at higher PCBM ratios. Yet, such optical scattering is not significant for P3HT/ICBA blends (even with high ICBA ratios). Overall, results here suggest the reported higher efficiencies of P3HT/ICBA solar cells (vs. P3HT/PCBM cells) cannot be attributed to larger and/or more ordered phase-separated donor–acceptor domains and other characteristics play more important roles in this case.

1. Introduction

Organic photovoltaics (OPVs) have attracted wide attention in recent years due to their potential advantages in fabrication, cost, and mechanical flexibility [1–3]. The energy conversion process in OPVs typically involves exciton generation upon light absorption, exciton diffusion and then dissociation of excitons into free carriers at the donor–acceptor (D–A) interface, and finally transport of carriers to their respective electrodes [1–3]. To achieve high conversion efficiencies, polymer bulk-heterojunctions (BHJ) composed of nanoscale interpenetrated (phase-separated) domains of donor and acceptor materials are introduced to increase areas of D–A interfaces for ensuring effective exciton diffusion to such interfaces, meanwhile providing transport paths for carrier transport/extraction to electrodes [4]. Among various D–A materials, poly(3-hexylthiophene) (P3HT) as a donor and [6,6]-phenyl-C_{61} butyric acid methyl ester (PCBM) as an acceptor are the most widely studied D–A combination [5–14], in considering light harvesting, carrier generation and carrier transport. Regioregular P3HT are known to have strong tendency of forming self-organized structure in thin films, which could be further enhanced upon appropriate treatments (e.g. thermal annealing, solvent annealing, etc.) [6–12]. More ordered molecular packing benefits charge transport (i.e., higher mobility) and absorption at longer wavelengths due to enhanced interchain interactions [6]. In BHJs, such treatments induce not only re-crystallization but also inter-diffusion of D/A

* Corresponding author. Tel.: +886 2 33663636; fax: +886 2 33669404.
E-mail address: chungwu@cc.ee.ntu.edu.tw (C.-C. Wu).

1566-1199/$ - see front matter © 2012 Elsevier B.V. All rights reserved.
http://dx.doi.org/10.1016/j.orgel.2012.07.023

components, giving some flexibility in tuning/optimizing nanoscale phase separation and interpenetration of donors and acceptors that is essential and critical to high-efficiency BHJ OPVs [13,14].

Recently, a few reports show that replacing PCBM with a new C_{60}-based acceptor material indene-C_{60} bisadduct (ICBA) in the P3HT/fullerene system could substantially improve the conversion efficiency of the solar cells [15–18]. Compared to PCBM, ICBA has more facile synthesis, higher solubility in common organic solvents, and stronger visible absorption for better light harvesting in the photovoltaic process. ICBA also exhibits a higher LUMO level than PCBM [15–18], which contributes to the higher open-circuit voltage of the P3HT/ICBA photovoltaic cell. In addition to the above properties, the detailed morphological properties of the donor–acceptor composites would also be essential in understanding the difference in performance between the P3HT/PCBM system and the relatively new P3HT/ICBA system. Although there have been numerous studies of the morphological properties of the P3HT/PCBM system, yet thus far the morphological study on the P3HT/ICBA system is sparse [19]. To acquire better understanding and useful information, in this work, a comparative study on morphological and related properties of the P3HT/PCBM and the P3HT/ICBA systems is conducted.

2. Experiments

2.1. Preparation of polymer/fullerene films

The structures of P3HT, PCBM, and ICBA used in this study are shown in Fig. 1. Regioregular P3HT(average molecular weight = 55–60 K, regioregularity = 95%, PDI$\sim$2.0), PCBM, ICBA were purchased from Rieke Metals Inc., Nano-C, and Luminescence Technology Corp., respectively, and were used as received. The pure or blend P3HT/fullerene solutions having different P3HT and fullerene weight ratios [P3HT: fullerene (PCBM or ICBA) = 1:0, 3:1, 2:1, 1:1, 1:2, 1:3, 0:1] were all prepared using chlorobenzene as the solvent and a total weight concentration of 20 mg/mL. The solutions were thoroughly stirred and shaken at the room temperature before use for film coating. Pure or blend thin-film samples of P3HT/fullerene for various studies were prepared by spin-coating (at $\sim$700 rpm) on Corning E2K glasses, with the average film thickness of $\sim$120 nm. For samples subjected to annealing, the annealing was conducted at 150 °C (the annealing temperature usually used for BHJ polymer solar cells) for 20 min.

2.2. Characterization of polymer/fullerene films

A UV–vis spectrophotometer (V-670, JASCO) equipped with an integrating sphere was used to characterize the transmittance, reflection and absorption spectra of pure or blend P3HT/fullerene films. Since some thin-film samples of P3HT/fullerene blends showed optical scattering properties, in this work, two types of transmittance were characterized: the total transmittance (T_{total}) and the direct transmittance (T_{direct}). T_{total} was measured by using a monochromatic light beam normally incident onto sample and then using an integrating sphere to collect transmitted light over all angles. On the other hand, T_{direct} was measured by using a monochromatic light beam normally incident onto the sample and then collecting transmitted light only in the normal direction (within a 5° collection angle). The difference between T_{total} and T_{direct} reveals whether the film is optically scattering. Similarly, two types of reflectance were characterized: the total reflectance (R_{total}) collected with the integrating sphere and the direct reflectance (R_{direct}) collected within a 5° collection angle. Since some thin-film samples of P3HT/fullerene blends showed optical scattering properties, the determination of optical absorption properties of films requires special attention. Instead of determining the actual absorptance (A) of various films from the normal transmittance directly (i.e., $A = 1-T_{direct}$), the absorptance A was determined by first measuring T_{total} and R_{total} and then by $A = 1-T_{total}-R_{total}$.

The morphologies and nanostructures (e.g. intermolecular structures and orientations etc.) of various pure and blend P3HT/fullerene films were investigated by grazing incidence X-ray scattering (GIXS). Compared to other conventional techniques of morphological characterizations (e.g. atomic force microscopy-AFM, scanning or transmission electron microscopy-SEM/TEM etc.), GIXS has the particular advantage of being able to provide structural/morphological information of a thin film at different scales [20–27], instead of being limited to just local observation or sample preparation (e.g. in AFM, SEM, TEM etc.). Fig. 2 illustrates the configuration of the GIXS measurement, which was conducted at the BL17A end station of the

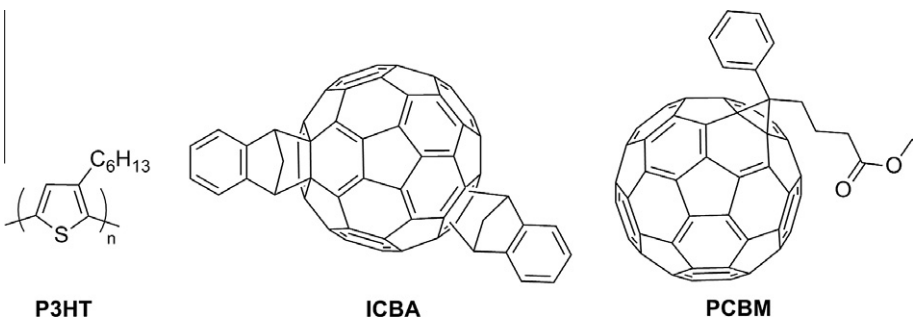

Fig. 1. Molecular structures of P3HT, ICBA, and PCBM.

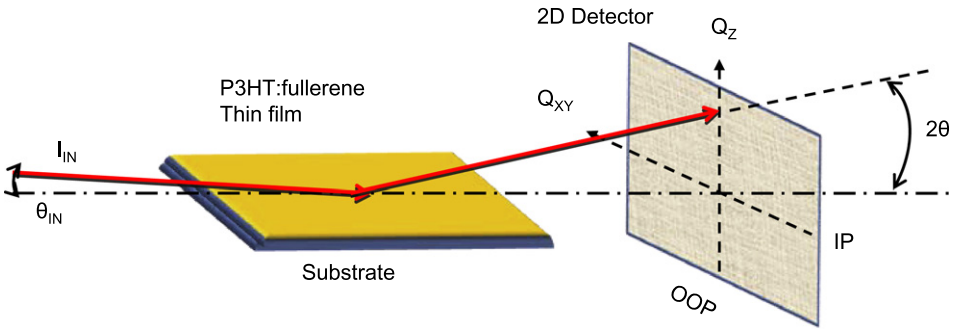

Fig. 2. Schematic illustration of the GIXS measurement. θ_{IN} denotes the incident angle, 2θ the diffraction angle, OOP the out-of-plane direction, and IP the in-plane direction. Q_{XY} and Q_Z are the components of the scattering vector along the IP and OOP directions, respectively.

National Synchrotron Radiation Research Center, Hsinchu, Taiwan. The 9.3-keV beam having a beam diameter of 1 mm was incident with and angle of incidence (θ_{IN}) of 0.1 degree. The 2D scattering images were collected by a MAR CCD detector array, with a sample-to-detector distance of 217 mm. The samples were kept at room temperature in air during irradiation and GIXS image collection. In Fig. 2, θ_{IN} denotes the incident angle, 2θ the diffraction angle (relative to the sample-detector axis), OOP the out-of-plane direction relative to the sample surface, and IP the in-plane direction relative to the sample surface. Q_{XY} and Q_Z are the components of the scattering vector Q along the IP and OOP direction, respectively, where $Q = 4\pi\sin(\theta)/\lambda$ and λ = the X-ray wavelength.

3. Results and discussion

3.1. Spectral properties and optical microscopy of pure and blend P3HT/fullerene films

Fig. 3 shows the absorption spectra of the pure and annealed P3HT, PCBM and ICBA thin films (with average thicknesses of ~120 nm).In general, P3HT shows strong absorption between 400 and 650 nm, while stronger absorption of PCBM and ICBA mainly occurs in the UV region. Compared to PCBM, ICBA exhibits stronger absorption in both the UV and visible regions, which is consistent with results of previous reports and is thought to be beneficial to light harvesting and photovoltaic conversion efficiencies [16,28].

In characterizing absorption spectra of P3HT/fullerene blend films of various ratios, initially a typical and straightforward approach of $A = 1 - T_{direct}$ (A = absorptance, T_{direct} = direct transmittance) was adopted. Fig. 4 shows the absorptance spectra of the various annealed pure and blend P3HT/PCBM films obtained this way. While these absorptance spectra roughly resemble the combination of P3HT and PCBM absorption, it is noticed that there is significant absorptance extended to wavelengths beyond 650 nm that does not exist in both pure P3HT and pure PCBM films. Since it occurred over a wide wavelength range, it was suspected that the blend films might possess optical scattering properties. This is plausible since the phase separation of the blend and the formation of interpenetrating domain networks would result in optically inhomogeneous films, which in turn could induce optical scattering if the domain sizes are comparable to optical wavelengths.

In consideration of the possibility of optical scattering, in addition to the more straightforward measurement of

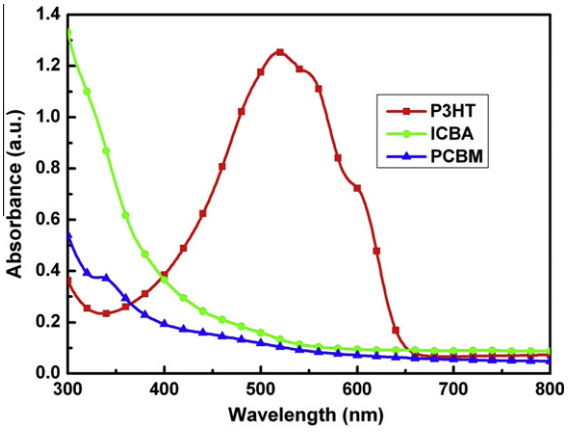

Fig. 3. Absorption spectra of pure P3HT, ICBA and PCBM films.

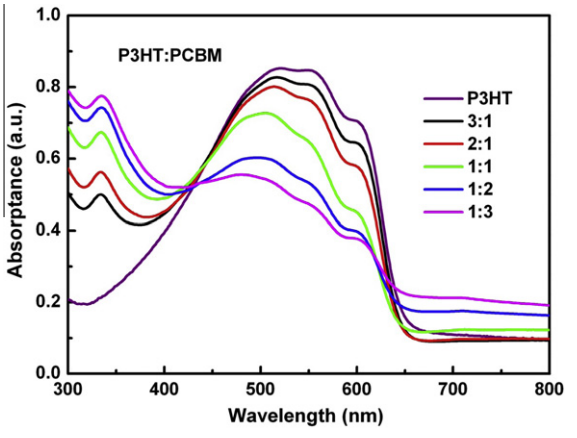

Fig. 4. Absorptance spectra of pure and blend P3HT:PCBM films extracted from the direct transmittance (T_{direct}).

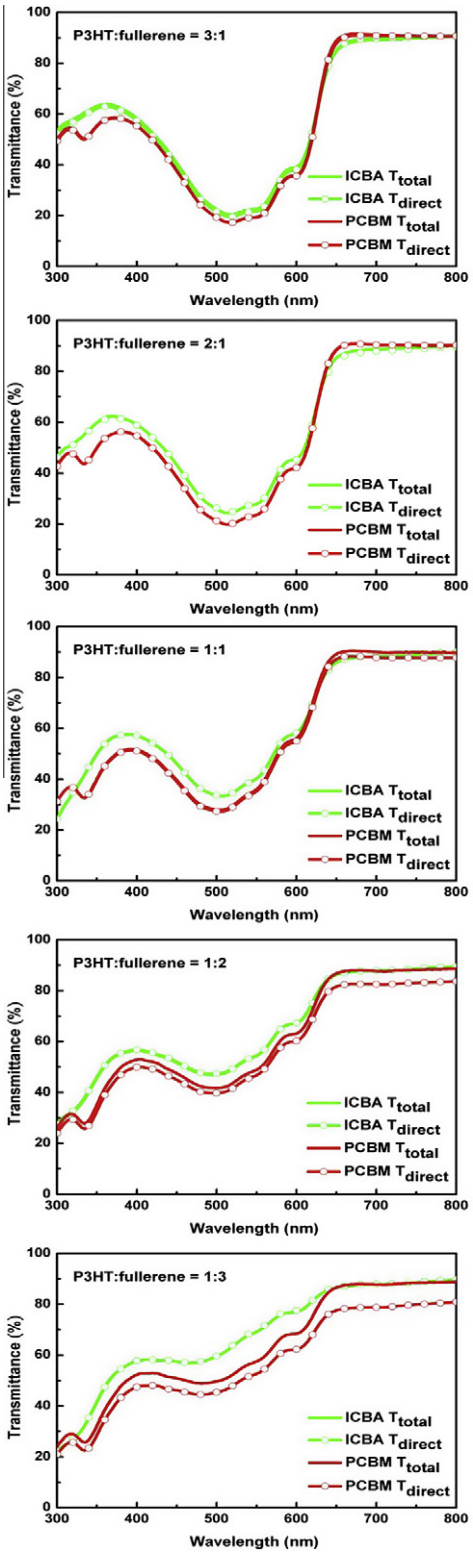

Fig. 5. Direct and total transmittance spectra of the P3HT:PCBM and P3HT:ICBA blend films having different P3HT:fullerene weight ratios.

direct transmittance T_{direct}, the total transmittance T_{total} was also measured using the integrating sphere. Fig. 5 shows the T_{direct} and T_{total} spectra of the P3HT/PCBM and the P3HT/ICBA blend films of various ratios. It is seen that while both T_{direct} and T_{total} spectra of P3HT/ICBA blend films remain rather close over the blend ratios investigated, yet larger differences in T_{direct} and T_{total} spectra are observed for P3HT/PCBM blend films having larger PCBM ratios. Such optical results strongly suggest larger phase-separation domains (and lower miscibility of component materials) in the P3HT/PCBM system (at least at higher PCBM ratios), compared to the P3HT/ICBA system.

Such a speculation indeed is supported by the optical microscopy (OM) observation of various P3HT/PCBM and P3HT/ICBA blend films. Fig. 6 shows the OM images of P3HT/PCBM and P3HT/ICBA blend films having different composition ratios. For the P3HT/PCBM system, in increasing the PCBM weight ratio to 50%, aggregate domains (under OM) becomes clearly visible, coincident with the appearing of the significant optical scattering in the transmittance spectra shown in Fig. 5. It had been reported that with increasing the PCBM fraction in the blend film, PCBM molecules tend to form larger clusters and leave larger depletion regions for recrystallization of P3HT [29]. Under annealing (thus with a driving force to accelerate PCBM diffusion and aggregation), PCBM clusters can grow up to a scale of tens to hundreds of micrometers in length [30], consistent with OM observations shown in Fig. 6. In contrast to the P3HT/PCBM system, in the OM images of the P3HT/ICBA blend films, there are no clearly visible phase-separation/aggregate domains under the OM resolution (i.e., ~100 nm), strongly suggesting the miscibility and morphologies in P3HT/ICBA blends could be very different from those of P3HT/PCBM blend films and explaining why the P3HT/ICBA blend films do not exhibit significant optical scattering (even up to a high ICBA weight ratio) as the P3HT/PCBM films.

By taking into account optical scattering properties of P3HT/fullerene films, the optical absorptance spectra of various pure and blend P3HT/PCBM and P3HT/ICBA films were carefully determined by first measuring the total transmittance T_{total} and the total reflectance R_{total} and then obtaining the actual absorptance A by $A = 1 - T_{total} - R_{total}$. Fig. 7(a) shows the absorptance spectra of various pure and blend P3HT/ICBA films, and Fig. 7(b) shows the absorptance spectra of various pure and blend P3HT/PCBM films. By comparing absorptance spectra of P3HT/PCBM in Fig. 7(b) and Fig. 4, one sees that by carefully taking into account optical scattering of blend films, all the absorptance spectra of pure and blend films now land on a same base line for wavelengths larger than 650 nm. The absorptance spectra thus obtained can now represent the true and actual absorption in films. The optical/spectral studies here thus have a significant implication. In studying the optical properties of BHJ polymer/organic solar cells, to obtain correct and physically meaningful results, it is crucial to take into account possible optical scattering effects, since BHJ is typically composed of donor and acceptor domains, which in turn implies potential optical inhomogeneity relative to the scale of optical wavelengths.

In both Fig. 7(a) and (b), distinct absorption from P3HT can be seen in P3HT/fullerene blend films with higher P3HT weight ratios. It has been known that the interchain

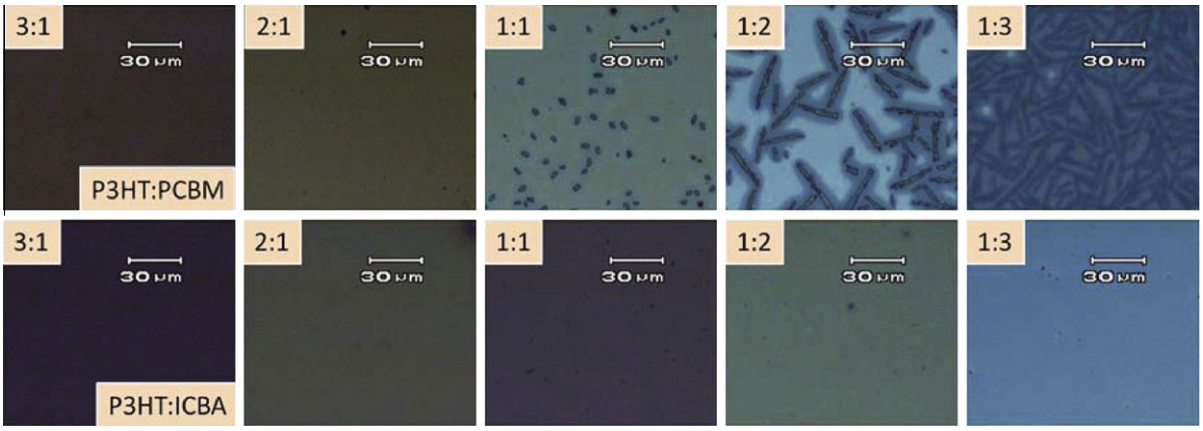

Fig. 6. OM images of the P3HT:PCBM and P3HT:ICBA blend films having different P3HT:fullerene weight ratios.

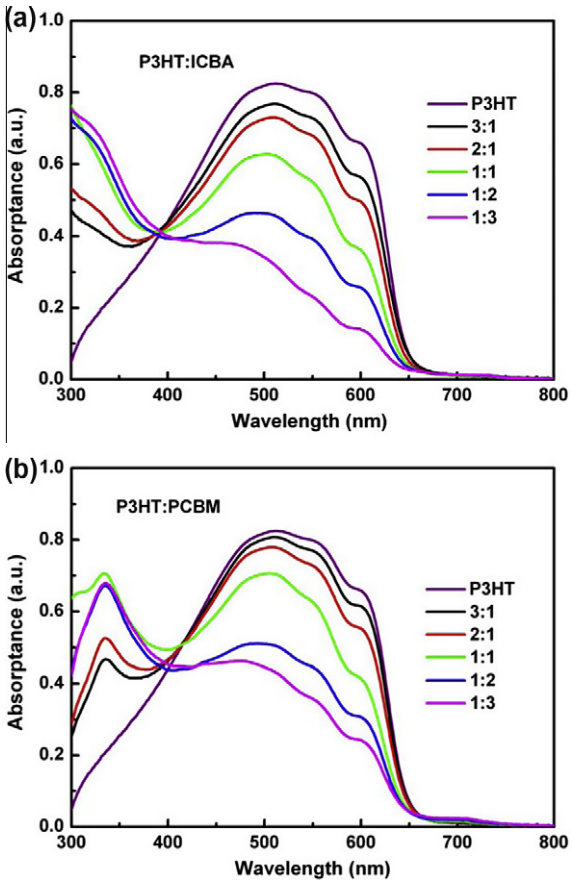

Fig. 7. Absorptance spectra of pure and blend (a) P3HT:ICBA, and (b) P3HT:PCBM films having different weight ratios.

interaction of P3HT results in more ordered polymer chain packing and gives rise to distinct vibronic features (e.g. between 600 and 500 nm etc., particularly longer-wavelength ones) in absorption spectra of P3HT films [13]. Thus the intensities of these P3HT vibronic features in absorption of blend films may somewhat reveal the overall crystallinities/ordering of P3HT in the blend films [31]. With reducing the weight ratios of P3HT, the absorption intensity from P3HT drops in both P3HT/PCBM and P3HT/ICBA films. However, a faster reduction of P3HT absorption is seen in the P3HT/ICBA blend films upon decreasing the P3HT weight ratio. It suggests that using ICBA as the acceptor appears to interfere or disrupt the interchain packing of P3HT more significantly than PCBM. To further understand such difference, GIXS was used to comparatively investigate the molecular packing/ordering, orientation, and crystallinity of pure and blend P3HT/PCBM and P3HT/ICBA films.

3.2. GIXS analyses of pure and blend P3HT/fullerene films

Fig. 8(a) shows the 2D GIXS images of the pure and annealed P3HT films. P3HT has a strong tendency to crystallize upon annealing and clear peaks associated with molecular packing are observed in the GIXS images. (100) and higher-order (200) and (300) reflections are associated with the lamella layer structure (i.e., layers of P3HT backbones/hexyl side chains), while the (010) reflection is associated with π–π interchain stacking (i.e., the face-to-face stacking of thiophene backbones) [32]. Fig. 8(a) reveals that the (100) axis is along the out-of-plane (OOP) orientation (i.e., normal to the substrate/film surface) and the (010) axis is along the in-plane (IP) orientation (i.e., in the plane of the substrate/film). Based on such GIXS patterns, Fig. 8(b) schematically illustrates the molecular packing structure in the self-organized, crystalline P3HT films. With hexyl side chains perpendicular to the substrate, such a stacking structure has the so-called edge-on orientation. The (100) reflection occurs at $|Q_Z| = 0.38\ \text{Å}^{-1}$ (i.e., $2\theta \sim 4.7°$), indicating a d-spacing of ~16.7 Å for P3HT lamellae. One also notices that there is a spread of the scattering patterns in the azimuthal manner, which is associated with the distribution of molecular inclination with respect to the substrate [33].

Fig. 9 shows 2D GIXS images of the as-coated and annealed films (annealed at 150 °C) of pure PCBM and ICBA. Both GIXS images of as-coated PCBM and ICBA films exhibit only broad and isotropic rings at $2\theta \sim 20°$, indicating

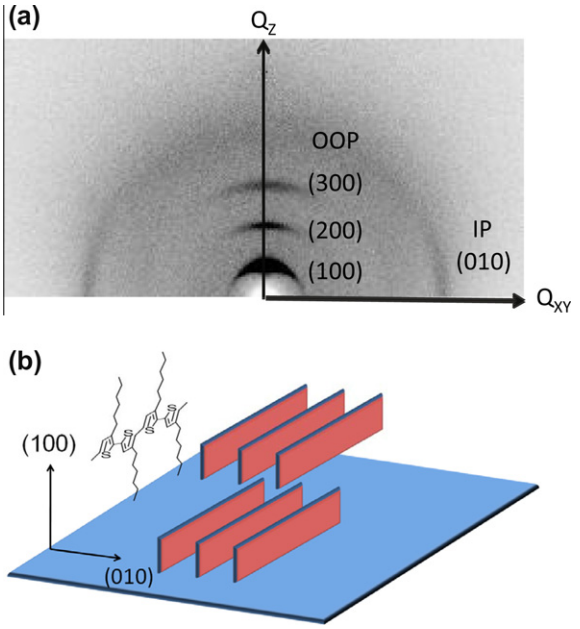

Fig. 8. (a) The 2D GIXS pattern of the pure and annealed P3HT film. (b) Schematic illustration of the lamellar stacking of P3HT chains in the edge-on orientation.

that both films are either amorphous or composed of very tiny crystallites as coated. After annealing, the PCBM film shows several distinct GIXS peaks, indicating crystallization of PCBM upon annealing. The appearing of GIXS peaks at certain specific locations (in the GIXS images) instead of being an isotropic ring indicates the crystallization occurs with preferential orientations. It further suggests the aggregation of PCBM molecules (during annealing) is associated with heterogeneous nucleation at the substrate interface [25]. In contrast to PCBM, the GIXS image of the annealed ICBA film still exhibits only a broad and isotropic ring, indicating ICBA molecules have much weaker tendency to aggregate and crystallize. Such results are consistent with spectral and OM studies of the P3HT/fullerene blend films (Figs. 5 and 6). This may be associated with the nature of the ICBA molecular structure, which is a bisadduct fullerene with two indene side groups. Depending on positions of two indene side groups, ICBA could have variety of isomer forms [34], whose distribution and variation could introduce disorder and perhaps would hinder aggregation/crystallization of ICBA molecules.

Fig. 10 shows the 2D GIXS images of P3HT/PCBM blend films with varied ratios. (100) and higher-order (200) and (300) reflections from P3HT are observed in samples of all blend ratios and still occur in the out-of-plane orientation. Such results indicate that in the P3HT/PCBM blend films, even to a high PCBM ratio, phase-separated P3HT domains still exhibit a self-assembled lamella structure with P3HT backbones roughly parallel to the substrate and the hexyl side chains perpendicular to the substrate (i.e., edge-on configuration), similar to the case of pure P3HT films. Nevertheless, the intensities of higher-order (200) and (300) reflections relative to that of the (100) reflection decrease

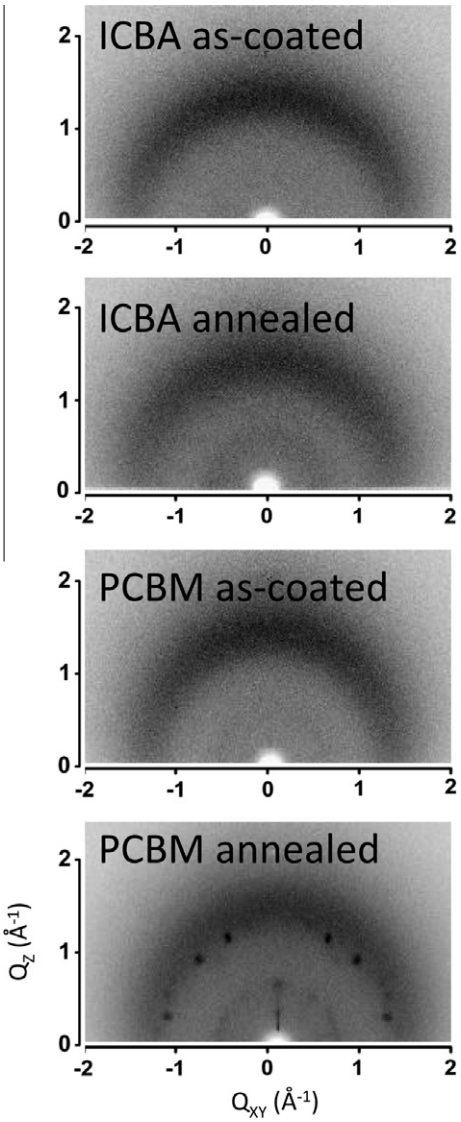

Fig. 9. 2D GIXS patterns of as-coated and annealed pure PCBM and ICBA films.

in increasing the PCBM ratio, suggesting the long-range order of P3HT crystallization is affected by appearance of PCBM. Meanwhile, with the PCBM ratio increased above 50%, the halo ring associated with PCBM exhibits some directional feature, indicating segregation and crystallization of PCBM with preferential orientations even in the blend films, consistent with OM and spectral observations discussed previously.

Fig. 11 shows the 2D GIXS images of P3HT/ICBA blend films. (100) and higher-order (200) and (300) reflections from P3HT are observed in the out-of-plane orientation in samples having lower ICBA ratios, indicating a lamella structure and an edge-on configuration. Yet one sees that the intensities of higher-order (200) and (300) reflections and even the (100) reflection drop rather fast in increasing the ICBA ratio. With the ICBA ratio above 50%, even the (100) reflection vanishes. Such results suggest that in the

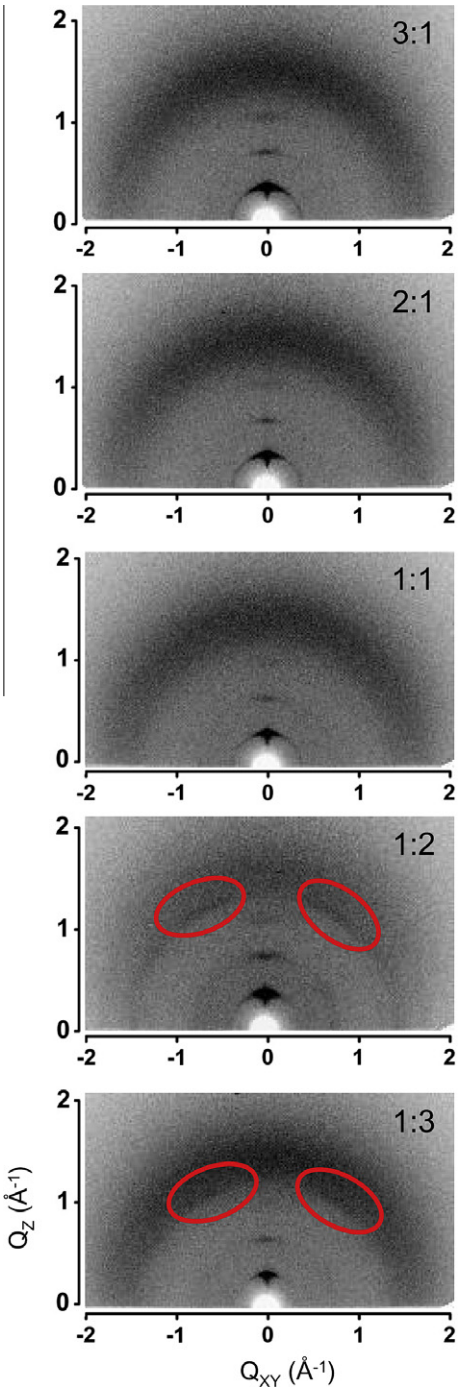

Fig. 10. 2D GIXS patterns of P3HT:PCBM blend films having different weight ratios.

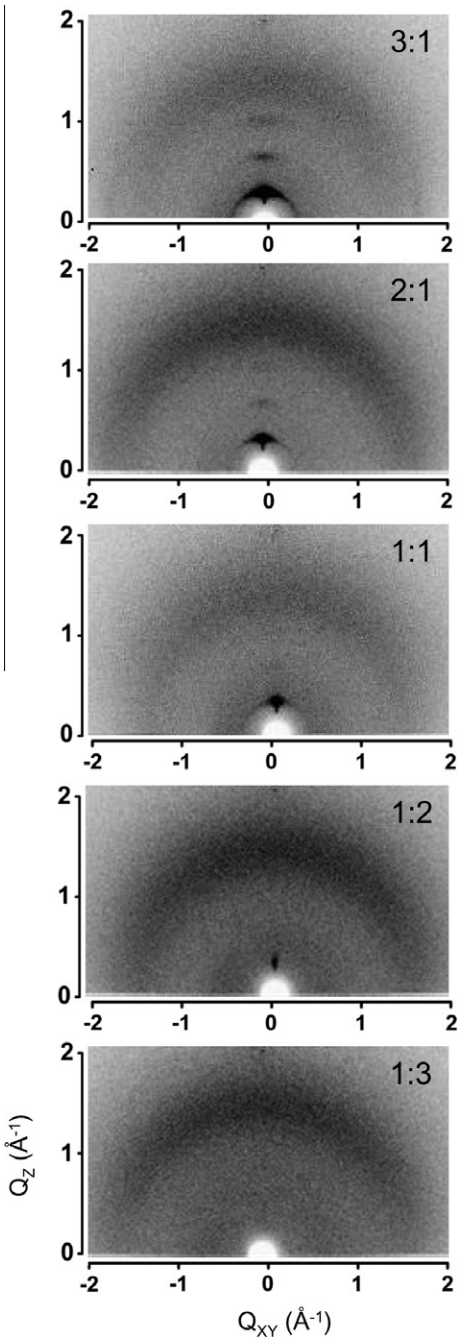

Fig. 11. 2D GIXS patterns of P3HT:ICBA blend films having different weight ratios.

P3HT/ICBA blends, the self-organization and packing of P3HT would be substantially disrupted by ICBA. Unlike the PCBM case, along with degradation of P3HT packing, the halo ring associated with ICBA still remains isotropic and does not reveal sign of crystallization or preferential orientation when increasing the ICBA ratio. Again, these characteristics are still attributed to the difference in molecular structures between PCBM and ICBA, which could intrinsically influence the diffusion/segregation and crystallization/aggregation capability of respective molecules. Depending on positions of two indene side groups, ICBA could have variety of isomer forms [34], whose distribution and variation could introduce disorder and perhaps would hinder aggregation/crystallization of P3HT and ICBA molecules themselves. With poorer organization/crystallization of P3HT in P3HT/ICBA blends, the lower intensity

of the 600-nm vibronic feature in the absorption spectra of the P3HT/ICBA blend films Fig. 7(a), which is associated with P3HT interchain interactions, could be understood.

Overall, from comparative GIXS morphological studies of various pure and blend films, one concludes that ICBA molecules exhibit weaker tendency to form larger and/or more organized domains in either pure or blend films, compared to PCBM. Furthermore, the presence of ICBA also interferes organization of P3HT and tends to degrade ordering and packing of P3HT in blend films. Such results suggest the reported higher efficiencies of P3HT/ICBA solar cells (vs. P3HT/PCBM cells) apparently cannot be attributed to larger and/or more ordered phase-separated donor and acceptor domains in the blends and other characteristics (e.g. different donor–acceptor energy-level alignment etc.) play more important roles in this case. It further suggests that larger and/or more ordered phase-separated donor and acceptor domains do not necessarily warrant higher performance in organic PVs. The morphological optimization conditions may vary among materials having different characteristics, depending on detailed tradeoffs between exciton diffusion, exciton dissociation, charge transport/extraction, and charge recombination etc. For instance, although the more ordered edge-on orientation is good for charge transport in the horizontal (in-plane or pi–pi stacking) direction, yet it is not good for vertical charge transport [35]. In that sense, the less ordered and/or smaller P3HT grains in P3HT/ICBA systems may indeed be beneficial for exciton dissociation (due to larger D–A interfacial areas) and be beneficial for charge transport along the vertical direction between electrodes. The weaker tendency of ICBA to segregate and to from larger organized domains may also have positive impacts to stability of BHJ solar cells, since it may prevent further phase separation and growth of D–A domains during device operation.

4. Conclusion

In conclusion, we report a comparative study on spectral and morphological properties of two blend systems for polymer solar cells: the donor material P3HT in combination with the acceptor material of either PCBM or ICBA that was reported to enhance efficiencies of polymer solar cells. Optical microscopy and grazing incidence X-ray scattering reveal the stronger tendency of PCBM to from larger and more ordered domains/grains than ICBA either in pure or blend films, while molecular structures/characteristics of ICBA appear to hinder its forming larger/more ordered domains/grains in pure and blend films. Compared to PCBM, the presence of ICBA also substantially perturbs the organization and longer-range ordering of P3HT in increasing the ICBA ratio in blends. With larger and more ordered phase-separated domains, the P3HT/PCBM blend films exhibit significant optical scattering at higher PCBM ratios. Yet, such optical scattering is not significant for P3HT/ICBA blends (even with high ICBA ratios). Overall, results here suggest the reported higher efficiencies of P3HT/ICBA solar cells (vs. P3HT/PCBM cells) cannot be attributed to larger and/or more ordered phase-separated donor–acceptor domains and other characteristics play more important roles in this case. It further implies the morphological optimization conditions may vary among materials having different characteristics.

Acknowledgements

The authors gratefully acknowledge the support from National Science Council (Grant NSC-99-2221-E-002-118-MY3), Ministry of Education (Grant 10R70607-2), and National Synchrotron Radiation Research Center (NSRRC) of Taiwan.

References

[1] H. Hoppe, N.S. Sariciftci, J. Mater. Chem. 16 (2006) 45.
[2] J. Peet, M.L. Senatore, A.J. Heeger, G.C. Bazan, Adv. Mater. 21 (2009) 1521.
[3] C.J. Brabec, J.R. Durrant, MRS Bull. 33 (2008) 670.
[4] N.S. Sariciftci, L. Smilowitz, A.J. Heeger, F. Wudl, Science 258 (1992) 1474.
[5] V. Shrotriya, E.H.E. Wu, G. Li, Y. Yao, Y. Yang, Appl. Phys. Lett. 88 (2006) 064104.
[6] R. Österbacka, C.P. An, X.M. Jiang, Z.V. Vardeny, Science 287 (2000) 839.
[7] F. Padinger, R.S. Rittberger, N.S. Sariciftci, Adv. Funct. Mater. 13 (2003) 85.
[8] G. Li, V. Shrotriya, Y. Tao, Y. Yang, J. Appl. Phys. 98 (2005) 043704.
[9] Y. Kim, S.A. Choulis, J. Nelson, D.D.C. Bradley, S. Cook, J.R. Durrant, Appl. Phys. Lett. 86 (2005) 063502.
[10] F.C. Chen, C.J. Ko, J.L. Wu, W.C. Chen, Sol. Energy Mater. Sol. cells 94 (2010) 2426.
[11] G. Li, Y. Yao, H. Yang, V. Shrotriya, G. Yang, Y. Yang, Adv. Funct. Mater. 17 (2007) 1636.
[12] F. Zhang, K.G. Jespersen, C. Björström, M. Svensson, M.R. Andersson, V. Sundström, K. Magunsson, E. Moons, A. Yartsev, O. Inganäs, Adv. Funct. Mater. 16 (2006) 667.
[13] G. Li, V. Shrotriya, J. Huang, Y. Yao, T. Moriarty, K. Emery, Y. Yang, Nat. Mater. 4 (2005) 864.
[14] H.N. Tsao, K. Müllen, Chem. Soc. Rev. 39 (2010) 2372.
[15] Y. He, H.Y. Chen, J. Hou, Y. Li, J. Am. Chem. Soc. 132 (2010) 377.
[16] G. Zhao, Y. He, Y. Li, Adv. Mater. 22 (2010) 4355.
[17] CJ. Brabec, A. Cravino, D. Meissner, N.S. Sariciftci, T. Fromherz, M.T. Rispens, L. Sanchez, J.C. Hummelen, Adv. Funct. Mater. 11 (2001) 374.
[18] Z.L. Guan, J.B. Kim, Y.L. Loo, A. Kahn, J. Appl. Phys. 110 (2011) 043719.
[19] N.C. Miller, S. Sweetnam, E.T. Hoke, R. Gysel, C.E. Miller, JA. Bartelt, X. Xie, M.F. Toney, M.D. McGehee, Nano Lett. 12 (2012) 1566.
[20] R.M. Beal, A. Stavrinadis, J.H. Warner, J.M. Smith, H.E. Assender, A.A.R. Watt, Macromolecules 43 (2010) 2343.
[21] R. Giridharagopal, D.S. Ginger, J. Phys. Chem. Lett. 1 (2010) 1160.
[22] M. Reyes-Reyes, K. Kim, J. Dewald, R. López-Sandoval, A. Avadhanula, S. Curran, D.L. Carroll, Org. Lett. 7 (2005) 5749.
[23] M. Sanyal, B. Schmidt-Hansberg, M.F.G. Klein, A. Colsmann, C. Munuera, A. Vorobiev, U. Lemmer, W. Schabel, H. Dosch, E. Barrena, Adv. Energy Mater. 1 (2011) 363.
[24] T. Agostinelli, S. Lilliu, J.G. Labram, M. Campoy-Quiles, M. Hampton, E. Pires, J. Rawle, O. Bikondoa, D.D.C. Bradley, T.D. Anthopoulos, J. Nelson, J.E. Macdonald, Adv. Funct. Mater. 21 (2011) 1701.
[25] E. Verploegen, R. Mondal, C.J. Bettinger, S. Sok, M.F. Toney, Z. Bao, Adv. Funct. Mater. 20 (2010) 3519.
[26] M. Sanyal, B. Schmidt-Hansberg, M.F.G. Klein, C. Munuera, A. Vorobiev, A. Colsmann, P. Scharfer, U. Lemmer, W. Schabel, H. Dosch, E. Barrena, Macromolecules 44 (2011) 3681.
[27] W.H. Baek, T.S. Yoon, H.H. Lee, Y.S. Kim, Org. Lett. 11 (2010) 933.
[28] J. Hou, H.Y. Chen, S. Zhang, G. Li, Y. Yang, J. Am. Chem. Soc. 130 (2008) 16144.
[29] A. Swinnen, I. Haeldermans, M. vandeVen, J. D'Haen, G. Vanhoyland, S. Aresu, M. D'Olieslaeger, J. Manca, Adv. Funct. Mater. 16 (2006) 760.
[30] V.D. Mihailetchi, H. Xie, B. de Boer, L.M. Popescu, J.C. Hummelen, P.W.M. Blom, L.J.A. Koster, Appl. Phys. Lett. 89 (2006) 012107.

[31] T. Erb, U. Zhokhavets, G. Gobsch, S. Raleva, B. Stühn, P. Schilinsky, C. Waldauf, C.J. Brabec, Adv. Funct. Mater 15 (2005) 1193.
[32] W. Ma, C. Yang, X. Gong, K. Lee, A.J. Heeger, Adv. Funct. Mater. 15 (2005) 617.
[33] M.L. Chabinyc, M.F. Toney, R.J. Kline, I. McCulloch, M. Heeney, J. Am. Chem. Soc.129 129 (2007) 3226.
[34] H. Kang, C.H. Cho, H.H. Cho, T.E. Kang, H.J. Kim, K.H. Kim, S.C. Yoon, B.J. Kim, ACS Appl. Mater. Interf. 4 (2012) 110.
[35] H. Sirringhaus, P.J. Brown, R.H. Friend, M.M. Nielsen, K. Bechgaard, B.M.W. Langeveld-Voss, A.J.H. Spiering, R.A.J. Janssen, E.W. Meijer, P. Herwig, D.M. de Leeuw, Nature 401 (1999) 685.